ADV MATH SCI JOURNAL
Advances in Mathematics: Scientific Journal **10** (2021), no.1, 517–526
ISSN: 1857-8365 (printed); 1857-8438 (electronic)
https://doi.org/10.37418/amsj.10.1.51 Spec. Issue on ICIRPS-2020

KELLER-BOX SOLUTION OF THE STAGNATION POINT MICROPOLAR FLUID FLOW BETWEEN POROUS PLATES WITH INJECTION

Ashwini Bhat[1] and Nagaraj N. Katagi

ABSTRACT. The present study deals with the steady axisymmetric flow of micropolar fluid between two parallel porous plates when the fluid is injected through both walls at the same rate. The influence of velocity slip at the porous surface is analyzed. A detailed finite-difference solution is developed for the resulting non-linear coupled differential equations representing velocities and microrotation. The numerical computations are obtained for radial, axial velocities, and microrotation for varying injection Reynolds number, micropolar parameter, and slip coefficient. Further, a comparison of the results is given with those obtained in the literature with different methods as special cases.

1. INTRODUCTION

The classical Navier-Stokes theory can not describe most natural and biological fluids with plenty of applications. Such liquids are named micropolar fluids [1] as a subclass of microfluids that comprises randomly arranged particles, which are also capable of rotating about their own axis and play a vital role in the dynamics of fluid flow. In 1966, Eringen mathematically formulated the governing equations for the motion of micropolar fluids in which, along with the velocity field, an equation representing microrotation was developed. Arimann [2] further confirmed the theory developed by Eringen. Using the fundamental

[1]*corresponding author*

2020 *Mathematics Subject Classification.* 00A79, 35A24.

Key words and phrases. Stagnation point flow, micropolar fluid flow, Slip velocity, Keller box method, Microrotation slip.

Submitted: 18.11.2020; *Accepted:* 25.12.2020; *Published:* 22.01.2021.

governing equations derived by Eringen, Wilson studied the two-dimensional micropolar boundary layer flow near the stagnation point. A finite-difference solution was also developed for the stagnation point boundary layer flow over a semi-infinite plate under steady conditions. Chapman and Bauer [3] gave an analytical solution for a steady stagnation point flow between two porous plates with constant blowing. Later, Agarwal and Dhanpal [4] obtained a numerical solution to the stagnation point micropolar fluid flow between two porous discs. Many other successful efforts can be found in the literature to understand the various stagnation point flow situations of Newtonian and non-Newtonian fluids using different approaches to find the solution.

However, it is noted that in most of the stagnation point micropolar fluid flow studies with porous boundaries, no-slip as well as no-spin boundary conditions are considered at the porous boundaries. The experimental studies conducted by Beavers and Joseph [5] concerning the flow at the interface of porous media and clear fluid shows the presence of velocity slip at the porous boundary. The historical background of these Beavers- Joseph conditions are also reported by Nield [6]. Later, these slip boundary conditions are successfully incorporated in the investigation of stokes and micropolar fluid flow situations between channels, tubes, and discs [7–9].

The fluid flow between porous parallel plates has received considerable attention due to its numerous application. Attempts have been made to research the various effects on the flow between plates under different boundary conditions. We proposed the impact of slip velocity on the stagnation point micropolar fluid flow between porous plates in the current investigation. Highly non-linear coupled governing equations are derived with suitable slip and spin boundary conditions. The system of governing equations and suitable boundary conditions are developed using a numerical technique based on the finite-difference approach called the Keller-box method. Keller [10] proposed this procedure over other traditional numerical techniques due to its unconditional stability. There are classical semi-analytical solution methods available to solve non-linear boundary value problems, but the challenges faced in selecting the initial solution and other parameters establishes that the proposed Keller-box method is a good alternative.

2. MATHEMATICAL FORMULATION

Consider two plates stationed at $\dot{z} = l$ and $\dot{z} = -l$ respectively as shown in figure (1). When an incompressible micropolar fluid is injected with uniform velocity through the plates, it flows radially towards center of the plane $\dot{z} = 0$. Considering planar symmetry of the problem we can effectively analyze upper half of the flow regime. Let (u, v, w) and (ν_1, ν_2, ν_3) are components of velocity and microrotation respectively in a cylindrical coordinate reference system. Due to axial symmetry the components of velocity and microrotation along radial, transverse and axial directions can be written as $u = u(\dot{r}, \dot{z}),\ v = 0,\ w = w(\dot{r}, \dot{z})$, $\nu_1 = \nu_3 = 0,$ and $\nu_2 = \nu(\dot{r}, \dot{z})$ respectively.

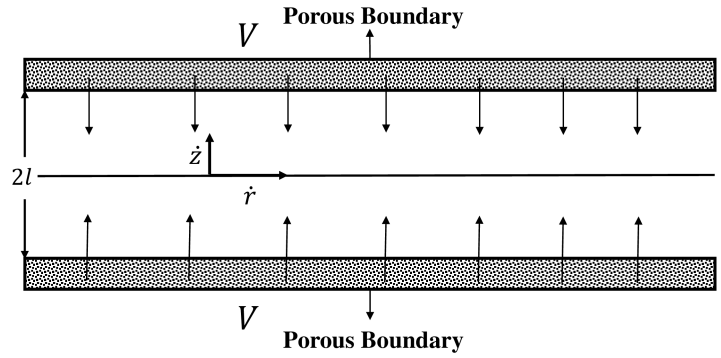

FIGURE 1. Geometry of micropolar fluid flow between porous plates

The governing equations are,

$$\frac{\partial u}{\partial \dot{r}} + \frac{u}{\dot{r}} + \frac{1}{l}\frac{\partial w}{\partial \chi} = 0$$

$$\rho\Big(u\frac{\partial u}{\partial \dot{r}} + \frac{w}{l}\frac{\partial u}{\partial \chi}\Big) = -\frac{\partial p}{\partial \dot{r}} - \frac{k}{l}\frac{\partial \nu}{\partial \chi} + (\mu + k)\Big(\frac{\partial^2 u}{\partial \dot{r}^2} + \frac{1}{\dot{r}}\frac{\partial u}{\partial \dot{r}} + \frac{1}{l^2}\frac{\partial^2 u}{\partial \chi^2} - \frac{u}{\dot{r}^2}\Big) \tag{2.1}$$

$$\rho\Big(u\frac{\partial w}{\partial \dot{r}} + \frac{w}{l}\frac{\partial w}{\partial \chi}\Big) = -\frac{1}{l}\frac{\partial p}{\partial \chi} - \frac{k}{\dot{r}}\frac{\partial}{\partial \dot{r}}\Big(\dot{r}\nu\Big) + (\mu + k)\Big(\frac{\partial^2 w}{\partial \dot{r}^2} + \frac{1}{\dot{r}}\frac{\partial w}{\partial \dot{r}} + \frac{1}{l^2}\frac{\partial^2 w}{\partial \chi^2}\Big) \tag{2.2}$$

$$\rho j\Big(u\frac{\partial \nu}{\partial \dot{r}} + \frac{w}{l}\frac{\partial \nu}{\partial \chi}\Big) = \gamma\Big(\frac{\partial}{\partial \dot{r}}\Big(\frac{\partial \nu}{\partial \dot{r}} + \frac{\nu}{\dot{r}}\Big) + \frac{1}{l^2}\frac{\partial^2 \nu}{\partial \chi^2}\Big) + k\Big(\frac{1}{l}\frac{\partial u}{\partial \chi} - \frac{\partial w}{\partial \dot{r}}\Big) - 2k\nu, \tag{2.3}$$

where $\chi = \frac{\dot{z}}{l}$ a non-dimensional variable, p is the pressure, ρ is the density, j is the constant microinertia, μ the viscosity, k and γ are the micropolar material constants. The boundary conditions for the velocity and microrotation in the

flow can be written as,

$$\text{At } \chi = 0,\ w(\dot{r},\chi) = \frac{\partial u}{\partial \chi} = 0,\ \nu(\dot{r},\chi) = \nu_0$$
$$\text{At } \chi = 1,\ w(\dot{r},\chi) = -V, u(\dot{r},\chi) = \frac{-\sqrt{\kappa}}{l\beta}\frac{\partial u}{\partial \chi}, \nu(\dot{r},\chi) = -\alpha\frac{\partial u}{\partial \chi},$$

where ν_0 represents the microrotation at center of the plane $\dot{z} = 0$, the slip coefficient is given by $\Phi = \frac{-\sqrt{\kappa}}{l\beta}$ where β is a dimensionless parameter that depends on porous material, κ is the permeability. α is a microrotation boundary parameter that measures the extent to which the microelements near the boundary are able to rotate. The value $\alpha = 0$ refers to the no-spin situation.

Defining stream function as,

$$\xi(\dot{r},\chi) = \frac{V\dot{r}^2}{2}F(\chi)$$
$$\text{So that } u = \frac{V\dot{r}}{2l}F(\chi) \tag{2.4}$$
$$w = -VF(\chi) \tag{2.5}$$

Further we take,

$$\nu = \frac{V\dot{r}}{2l^2}G(\chi) \tag{2.6}$$

Substituting (2.4)-(2.6) into (2.1-2.3) and upon eliminating p, we get

$$\frac{2(1+r)}{Re}F^{iv} - 2FF''' - \frac{r}{Re}G'' = 0 \tag{2.7}$$
$$AG'' + BRe\Big(\frac{1}{2}F'G - FG'\Big) = \frac{2r}{A}(G - F'') \tag{2.8}$$

Where, $r = \frac{k}{\mu}$ is the micropolar parameter, $A = \frac{\gamma}{\mu l^2}$ and $B = \frac{j}{l^2}$ are the micropolar constants and $Re = \frac{lV\rho}{\mu}$ is the suction/injection Reynolds number.

The transformed set of boundary conditions are,

$$F(0) = F''(0) = 0,\ \ G(0) = G_0$$
$$F(1) = -1,\ \ F'(1) = -\Phi F''(1),\ \ G(1) = \alpha F''(1) \tag{2.9}$$

The expressions for shear stress and couple stress at the porous plate boundary can be derived as,

$$\tau = -(\mu + k)\Big(\frac{\partial u}{\partial \dot{z}}\Big)_{\dot{z}=l} = -\mu(1+r)\frac{\dot{r}V}{2l^2}F''(1)$$
$$\Gamma = -\gamma\Big(\frac{\partial \nu}{\partial \dot{z}}\Big)_{\dot{z}=l} = -\gamma\frac{\dot{r}V}{2l^3}G'(1)$$

3. Results and discussion

The system of non-linear coupled ordinary equations represented by (2.7) and (2.8) for different values of micropolar parameter r and Reynolds number Re subjected to boundary conditions (2.9) are solved using numerical method based on Newtons linearisation technique. The solution procedure uses finite difference approximations and solves over a box scheme, is also called Keller-box technique. The method is used as described by Keller [10]. For better understanding, the numerical results for velocity and microrotation of the current flow situation are obtained corrected to 6 decimals for various values of r and Re and are plotted in figures(2)-(5). It is also observed that the variations in micropolar parameters A and B doesn't significantly effect the velocity and microrotation profiles and thus throughout the analysis these values are fixed at 1.0 and 0.001 respectively.

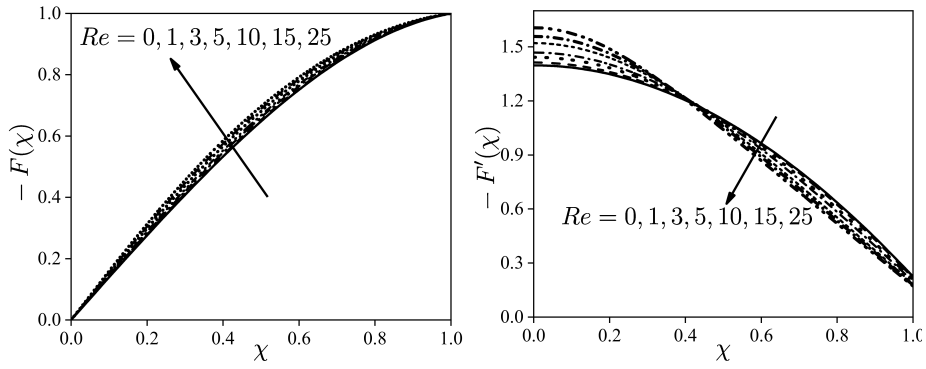

(a) (b)

FIGURE 2. Plots of (a)axial and (b)radial velocity for different Reynolds number Re with $r = 1, \Phi = 0.1, \alpha = 0.2, G_0 = 0$

Figures (2(a)) and (2(b)) depicts the variations in velocity components for change in Reynolds number for fixed values of other parameters in the flow. The axial velocity component increases throughout the flow regime for an increase in Reynolds number. But the magnitude of radial velocity component increases near the center of the distance between plates for increase in Reynolds number and a gradual decrease is observed near the porous plate.

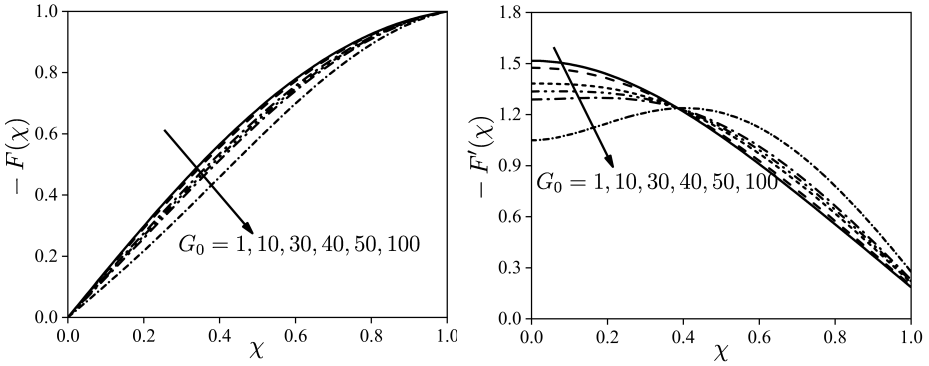

FIGURE 3. Plots of (a)-axial and (b)-radial velocity for different values of G_0 with $r = 1, Re = 10, \Phi = 0.1, \alpha = 0.2$

Figures (3(a)) and (3(b)) reveals the effect of arbitrary values of microrotation at the central plane on velocity vectors. G_0 has positive effect on the axial velocity in flow regime, while the radial velocity increases near the central plane, a transition is observed close to the stagnation point and the magnitude of radial velocity is seen decreasing in the vicinity of permeable plate. Further, the variations in microrotation of the flow elements are depicted in figure-4(a) for different G_0. Larger the value of G_0, it is clear from the figure that magnitude of microrotation decreases significantly from the central plane to the boundary. Combined effects of micropolar parameter and Reynolds number on the microrotation profile is visualized in figure (4(b)).

The presence of slip coefficient at the boundary influences flow characteristics, the plots of velocity and microrotation profiles for different values of Φ are shown in figure (5). As expected, the axial velocity decreases with increase in slip parameter, varying from 0 to 1 across the distance between plates. Though

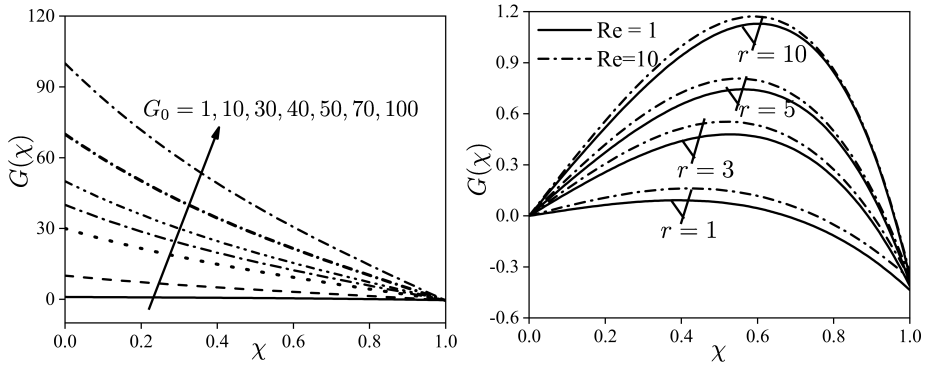

FIGURE 4. (a)Microrotation profile for different values of micropolar parameter G_0 with $r = 1, Re = 10, \Phi = 0.1, \alpha = 0.2$ (b) Microrotation profile for different values of micropolar parameter r and Reynolds number Re with $\Phi = 0.1, \alpha = 0.2, G_0 = 0$

TABLE 1. Comparison of the literature and present results for no-slip case with $r = 0, \Phi = 0$

χ	Re=0.1				Re=10			
	Chapman & Bauer [3]		Present		Chapman & Bauer [3]		Present	
	$-F(\chi)$	$-F(\chi)$	$-F'(\chi)$	$-F'(\chi)$	$-F(\chi)$	$-F(\chi)$	$-F'(\chi)$	$-F'(\chi)$
0	0.000000	0.000000	1.503417	1.503411	0.000000	0.000000	1.706711	1.706727
0.1	0.149832	0.149833	1.488210	1.488215	0.169533	0.169533	1.672930	1.672929
0.2	0.296624	0.296627	1.442609	1.442604	0.332492	0.332499	1.576930	1.576938
0.3	0.437338	0.437338	1.366684	1.366683	0.483284	0.483286	1.432194	1.432196
0.4	0.568948	0.568947	1.260546	1.260545	0.617837	0.617841	1.254715	1.254716
0.5	0.688440	0.688442	1.124345	1.124348	0.733592	0.733600	1.058123	1.058135
0.6	0.792817	0.792820	0.958271	0.958276	0.829136	0.829136	0.851680	0.851685
0.7	0.879101	0.879109	0.762543	0.762540	0.903778	0.903779	0.640673	0.640673
0.8	0.944340	0.944335	0.537408	0.537409	0.957208	0.957210	0.427727	0.427767
0.9	0.985606	0.985604	0.283134	0.283135	0.989298	0.989302	0.214010	0.214040
1	1.000000	1.000000	0.000000	0.000000	1.000000	1.000000	0.000000	0.000000

the magnitude of radial velocity initially decreases near the central plane, a complete opposite behavior is observed as the boundary is reached with the flow transition happening exactly at the critical point for different values of Φ. The boundary layer thickness is thinner than no-slip case($\Phi = 0$) and the velocity profiles are benign.

Since the experimental data and the analytical solution for the considered flow situation is unavailable, the exact comparison is not possible. However, we compared the results with that for viscous case in the absence of micropolar parameters and no-slip conditions [3] in table (1).

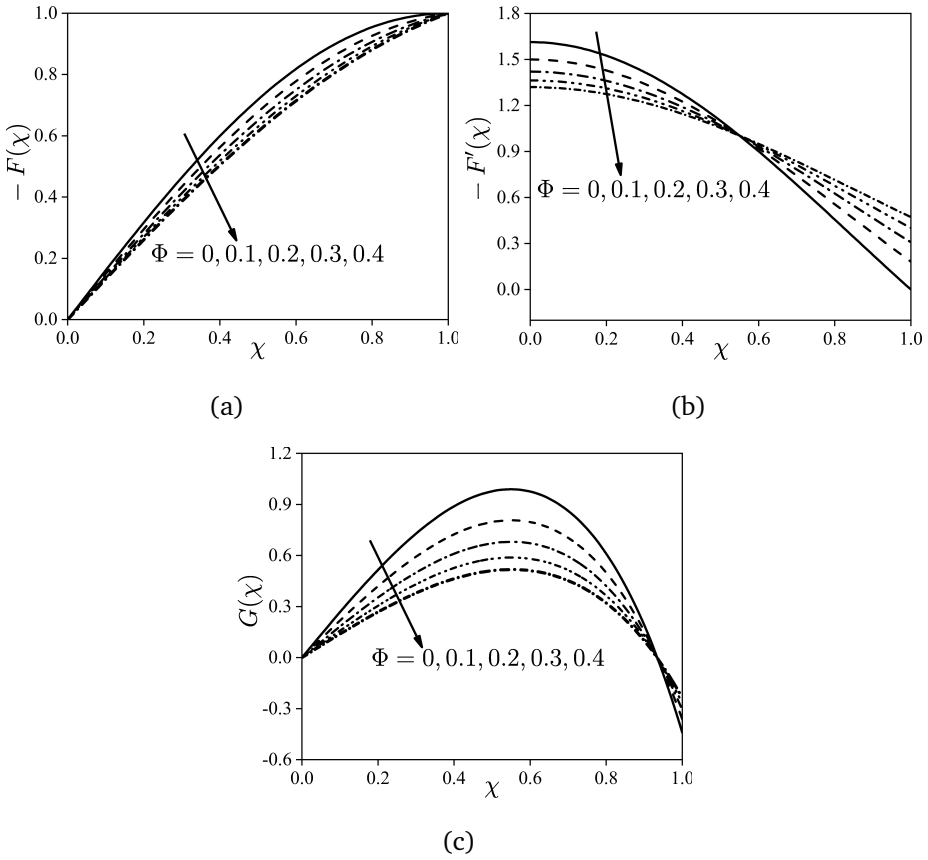

FIGURE 5. (a)Axial, (b)radial, and (c)microrotation profiles for various values of velocity slip parameter Φ with $r = 5, Re = 10, G_0 = 0, \alpha = 0.2$

TABLE 2. Numerical solution for skin friction coefficient $F''(1)$

r	$\Phi = 0, s = 0, G_0 = 0$					
	$Re = 0$	$Re = 1$	$Re = 3$	$Re = 5$	$Re = 10$	$Re = 25$
0	2.970074	2.755865	2.468101	2.305831	2.140709	2.048535
1	2.890199	2.779379	2.598333	2.462487	2.257776	2.083459
5	2.542645	2.508429	2.445302	2.388808	2.273199	2.081541
10	2.321804	2.304147	2.270589	2.239285	2.170193	2.027477
r	$\Phi = 0.1, s = 0.2, G_0 = 1$					
	$Re = 0$	$Re = 1$	$Re = 3$	$Re = 5$	$Re = 10$	$Re = 25$
0	2.284659	2.163303	1.989478	1.884479	1.770437	1.703005
1	2.246740	2.183251	2.075612	1.991160	1.856298	1.731018
5	2.078001	2.055940	2.014581	1.976788	1.896786	1.752984
10	1.967054	1.954370	1.930003	1.906945	1.854807	1.739870

TABLE 3. Numerical solution obtained for couple stress coefficient $-G'(1)$

r	$\Phi = 0, s = 0, G_0 = 0$					
	$Re = 0$	$Re = 1$	$Re = 3$	$Re = 5$	$Re = 10$	$Re = 25$
0	0.000000	0.000000	0.000000	0.000000	0.000000	0.000000
1	1.715231	1.713269	1.709386	1.705694	1.697799	1.683664
5	6.085842	6.069745	6.038834	6.009637	5.943997	5.802082
10	9.301820	9.278456	9.233036	9.189349	9.087559	8.840932
r	$\Phi = 0.1, s = 0.2, G_0 = 1$					
	$Re = 0$	$Re = 1$	$Re = 3$	$Re = 5$	$Re = 10$	$Re = 25$
0	1.461547	1.435006	1.397256	1.374399	1.348375	1.326303
1	2.770326	2.758710	2.738541	2.722092	2.693533	2.656776
5	6.415041	6.401711	6.375784	6.350892	6.293471	6.162025
10	9.454297	9.434801	9.396537	9.359271	9.270631	9.044562

Tables (2) and (3) represents numerical computation results obtained for shear stress coefficient and couple stress coefficient at the permeable wall for different Reynolds number and micropolar parameter. It can be easily observed from the values that, the presence of micropolar elements decreases the shear stress but, it increases couple stress. Further, for fixed values of other parameters, the magnitude of skin friction decreases and the wall couple stress increases. The similar effects are observed with increase in spin parameter.

REFERENCES

[1] A.C. ERINGEN: *Theory of micropolar fluids*, Journal of Math. Mech., **16**(1) (1966), 1–18.

[2] T.ARIMAN, M.A. TURK, N.D. SYLVESTER: *Micro continum fluid mechanics a review*, International Journal of Engineering Science, **11** (1973), 905–930.

[3] T.W. CHAPMAN, G.L. BAUER: *Stagnation-point viscous flow of an incompressible fluid between porous plates with uniform blowing*, Appl. Sci. Res., **31** (1975), 223–239.

[4] R.S. AGARWAL, C.DHANPAL: *Stagnation point micropolar fluid flow between porous discs with uniform blowing*, Int. J. Engg. Sci., **26** (1988), 293–300.

[5] S.GORDON BEAVERS, D.DANIEL JOSEPH: *Boundary conditions at a naturally permeable wall*, Journal of Fluid Mechanics, **30** (1967), 197–207.

[6] D.A. NIELD: *The beavers-joseph boundary condition and related matters: A historical and critical note*, Transport in Porous Media, **78** (2009), 537–540.

[7] S.RAJINDAR, L.LAURENCE, ROBERT: *Influence of slip velocity at a membrane surface on ultrafiltration performance - I. Channel flow system*, Int. J. Heat and Mass Transfer, **22** (1979), 721–729.

[8] S.RAJINDAR, L.LAURENCE ROBERT: *Influence of slip velocity at a membrane surface on ultrafiltration performance - II. Tube flow system*, Int. J. Heat and Mass Transfer, **12** (1979), 731–737.

[9] B.ASHWINI, N.K. NAGARAJ: *Micropolar fluid flow between a non-porous disk and a porous disk with slip: Keller-box solution*, Ain Shams Engineering Journal, **11**(1) (2000), 149–159.

[10] H.B. KELLER: *Numerical methods in boundary layer theory*, Ann. Rev. Fluid. Mech., **10** (1978), 417–433.

DEPARTMENT OF MATHEMATICS, MANIPAL INSTITUTE OF TECHNOLOGY,
MANIPAL ACADEMY OF HIGHER EDUCATION, MANIPAL-576104, INDIA.
Email address: ashwini.bhat@manipal.edu

DEPARTMENT OF MATHEMATICS, MANIPAL INSTITUTE OF TECHNOLOGY,
MANIPAL ACADEMY OF HIGHER EDUCATION, MANIPAL-576104, INDIA.
Email address: nn.katagi@manipal.edu